

Paweł WYSMULSKI
Hubert DĘBSKI
Patryk RÓŻYŁO
Katarzyna FALKOWICZ

A STUDY OF STABILITY AND POST-CRITICAL BEHAVIOUR OF THIN-WALLED COMPOSITE PROFILES UNDER COMPRESSION

BADANIA STATECZNOŚCI I STANÓW POKRYTYCZNYCH ŚCISKANYCH CIENKOŚCIENNYCH PROFILI KOMPOZYTOWYCH*

The object of this study is a thin-walled channel-section profile made of a carbon-epoxy composite subjected to axial compression. The study included analysis of the critical and weakly post-critical behaviour using experimental and numerical methods. As a result of the research conducted on a physical model of the structure, we determined a post-critical equilibrium path, which was then used to determine the critical load by approximation methods. Simultaneously, numerical calculations were performed by the finite element method. Their scope included a linear analysis of eigenvalue problems, the results of which led to determination of the critical load for the developed numerical model. The second step of the calculations consisted in performing a nonlinear analysis of the structure with geometrically initiated imperfection corresponding to the lowest buckling mode of the investigated profile. The numerical results were compared with the experimental findings, revealing that the developed numerical model of the structure was correct. The numerical simulations were performed using the ABAQUS® software.

Keywords: *finite element method, stability of construction, composites, critical state, thin-walled structures.*

Przedmiotem badań jest cienkościenny profil o przekroju ceowym, wykonany z kompozytu węglowo-epoksydowego, poddany osiowemu ścisnaniu. Zakres badań obejmował analizę stanu krytycznego i słabo pokrytycznego metodami doświadczalnymi i numerycznymi. W wyniku badań prowadzonych na fizycznym modelu konstrukcji wyznaczono pokrytyczną ścieżkę równowagi, na podstawie której z wykorzystaniem metod aproksymacyjnych określono wartość obciążenia krytycznego. Równolegle prowadzono obliczenia numeryczne z wykorzystaniem metody elementów skończonych. Zakres obliczeń obejmował liniową analizę zagadnienia własnego, w wyniku której określono wartość obciążenia krytycznego modelu numerycznego konstrukcji. Drugi etap obliczeń obejmował nieliniową analizę stanu słabo pokrytycznego konstrukcji z zainicjowaną imperfekcją geometryczną, odpowiadającą najniższej postaci wyboczenia konstrukcji. Wyniki obliczeń numerycznych porównano z wynikami badań doświadczalnych, potwierdzając adekwatność opracowanego modelu numerycznego konstrukcji. Zastosowanym narzędziem numerycznym był program ABAQUS®.

Słowa kluczowe: *metoda elementów skończonych, stateczność konstrukcji, kompozyty, stan krytyczny, konstrukcje cienkościenne.*

1. Introduction

Thin-walled load-carrying structures are characterized by high stiffness and strength compared to their specific weight. Owing to these properties, thin-walled elements are widely used in many industrial branches, particularly in the aerospace and automotive industry. This especially pertains to thin-walled profiles with complex shapes of the cross section which are used as stiffening elements. The disadvantage of such structures is that they can lose stability even under operational load [8, 15, 16]. When the buckling of a thin-walled element is local and elastic, the structure does not get damaged, and the element itself can be safely operated in the post-critical state [5, 15, 16, 23]. Given the above, the data regarding the critical load at stability loss of a thin-walled structure is of vital significance to the structure's operation. Unfortunately, the methods for determining the critical load of real structures are not unequivocal, which adds up to the difficulty with respect to a rational design of such structures. This being the case, an alternative tool enabling determination of critical

load is performing a numerical analysis by the finite element method [13, 15, 16]. Critical load is determined using a nonlinear eigenproblem analysis based on the minimum potential energy of the system. The numerically determined critical load can be to a certain extent regarded as determination of the critical force due to the fact that such computations are performed for an ideal structure which does not take account of geometric defects occurring in real structures. This means that the numerical models of thin-walled structures with complex cross-sectional shapes should be validated in experimental tests. Such a procedure will lead to a development of adequate discrete models enabling analysis of the complex problem of stability loss and post-critical behaviour of thin-walled structures [4, 6, 9, 10, 16, 26].

In the design of modern thin-walled structures used in state-of-the-art aircraft or automotive structures, traditional engineering materials (metals) are replaced by advanced composite materials. Given the structure of composites, this predominantly pertains to composite materials known as laminates [2, 3, 14, 17, 25, 27, 28, 29], or laminar composites. These materials exhibit a high strength to specific weight

(*) Tekst artykułu w polskiej wersji językowej dostępny w elektronicznym wydaniu kwartalnika na stronie www.ein.org.pl

ratio, which makes them widely used in load-carrying structures. An additional advantage of composite materials is the fact that we can shape their mechanical properties as desired by selecting a specified set of material properties and laminate lay-up arrangement. The literature on thin-walled load-carrying structures made of composite materials is rather scarce, the majority of publications being devoted to theoretical issues, while there are very few publications reporting experimental results.

The purpose of this study is to investigate the behaviour of a thin-walled, channel-section carbon/epoxy composite profile under axial compression in both critical and weakly post-critical state. The study involves determination of the critical load of a real structure as well as analysis of the critical and post-critical states by the finite element method. The study also presents a methodology for solving the problem of buckling and nonlinear stability of thin-walled structural elements made of composite materials.

2. Object of the study

The study was performed on a short thin-walled channel-section profile under axial compression. The investigated profile is a standard thin-walled structure consisting of perpendicular walls in the form of flat plates which are joined on longer edges [5, 6, 23]. The structure was produced by autoclave and it was made of a carbon/epoxy composite denoted as M12/35%/UD134/AS7/143. The composite lay-up consisted of 8 layers in a symmetric arrangement relative to the central plane described by the configuration $[0/-45/45/90]_s$. The channel-section profile

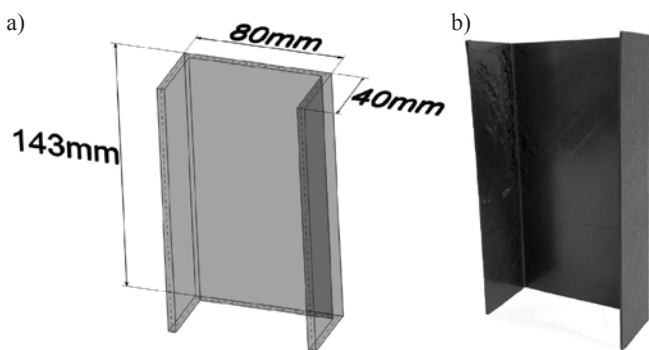


Fig. 1. Thin-walled channel-section column: a) geometric model, b) physical model of the structure

Table 1. Mechanical properties of carbon/epoxy composite

Young's modulus [GPa]		Poisson's ratio ν_{12}	Kirchhoff's modulus G_{12} [GPa]
$0^\circ (E_1)$	$90^\circ (E_2)$		
130.71	6.36	0.32	$\pm 45^\circ$
			4.18

had the overall dimensions of 80x40 mm, a wall thickness of 0.148 mm and a length of 143 mm – Fig. 1.

Basic mechanical properties of the produced composite material were determined in experimental tests according to the relevant ISO standard [19, 20, 21]. Thereby determined mechanical properties of the carbon/epoxy composite allow us to define a model of the material with orthotropic properties in a two-dimensional state of stress (Table 1).

3. Methods and scope of the study

The study involved both experimental and numerical investigation of the critical and weakly post-critical state of a thin-walled composite structure under compression. The experimental tests conducted on the



Fig. 2. Test stand used in the experiments

produced thin-walled composite columns enabled observing the real behaviour of the structure in a critical state and its operation following the stability loss. The purpose of the parallel-run numerical analysis was to develop adequate, experimentally validated FEM models for investigating the problem of stability (critical state) of thin-walled composite structures; in other words, models that would accurately reflect the behaviour of a real structure.

3.1. Experimental

The experimental tests were performed on a thin-walled composite profile with a channel section for a load range of approx. 150% of the critical force determined in the numerical simulation. The experiments were performed in room temperature on the Zwick Z100 universal testing machine with a maximum load range of 100 kN, at a constant speed of the upper cross beam set to 2 mm/min. In the tests, the profile ends were simple-supported to ensure articulate support of individual profile walls which had the form of plate elements. To prevent the impact of boundary conditions on the structure, both ends of the profile were provided with soft material pads to level potential inaccuracies of the end sections of the profile. The specimen was aligned using special pads enabling precise setting of the profile's end sections relative to the bolts of the testing machine. The test stand with the mounted specimen is shown in Fig. 2.

The experiments involved measuring variations in the compressive force and strains using strain gauges located lengthwise the column on the opposite sides of the web in the region of the highest expected deflection. The obtained post-critical equilibrium paths describing the relationship between load and difference in strain, $P-(\varepsilon_1-\varepsilon_2)$, enabled determination of the critical load as well as assessment of the structure's behaviour in a weakly post-critical range.

3.2. Approximation methods for determining critical load in experiments

Inaccuracies occurring in experimental tests due to various independent factors such as geometric defects of the structure, design of the test stand, load and boundary conditions hamper accurate determi-

nation of critical load. In such cases, it is necessary to use approximation methods which enable assessing the critical load based on experimental results. The assessment of the critical force was performed by two independent approximation methods: Koiter's method and the $P-w^2$ method [18].

The application of Koiter's method consisted in approximation of the post-critical equilibrium path describing the relationship between the specimen's load and the difference in strains measured on the opposite sides of the profile wall. Here, the experimentally determined post-critical equilibrium path, $P-(\varepsilon_1-\varepsilon_2)$, in a weakly post-critical range is approximated with a quadratic function expressed as [18]:

$$P = P_{cr} \frac{\alpha_2}{\alpha_0} w^2 + P_{cr} \frac{\alpha_1}{\alpha_0} w + P_{cr} \quad (1)$$

where: $\alpha_0, \alpha_1, \alpha_2$ are unknown parameters of the function, P is the applied force, P_{cr} is the unknown critical load, and $w \approx (\varepsilon_1 - \varepsilon_2)$ denotes the increase in deflection measured perpendicular to the profile wall.

In Koiter's method, the critical load is a point of intersection of function (1) and the vertical axis of the coordinate system describing the post-critical behaviour of the structure, $P-(\varepsilon_1-\varepsilon_2)$. The accuracy of the determined critical load depends on selection of an approximation range, where, in the case of stable behaviour of the structure, the direction coefficient of the second-order polynomial must be positive.

With the $P-w^2$ method, the critical load is also determined based on the post-critical equilibrium path; however, the assessment of the approximate value of critical force is done based on the relationship between load and the square of deflection perpendicular to the plane of the profile wall. In this study, the deflection w was approximated by a difference in the results obtained with the strain gauges ($\varepsilon_1-\varepsilon_2$). The post-critical equilibrium path $P-w^2$ was approximated by a linear function expressed as [18]:

$$P = P_{cr} \frac{\alpha_1}{\alpha_0} w + P_{cr} \quad (2)$$

where: α_0, α_1 are unknown parameters of the function, P is the applied force, P_{cr} is the value of unknown critical load, and $w^2 \approx (\varepsilon_1 - \varepsilon_2)^2$ denotes the increase in deflection measured perpendicular to the profile wall.

The critical load is a point of intersection of approximation function (2) and the vertical axis of the coordinate system describing the post-critical behaviour of the structure, $P-(\varepsilon_1-\varepsilon_2)^2$.

The approximation results obtained with the above methods are not always unequivocal. The degree of linearity of the approximated curve is inextricably linked to the range of data used for determining critical loads. In addition, the results significantly depend on the number of points described by specified coordinates subjected to approximation.

In the experiments, the key factor describing the accuracy of approximation was a correlation coefficient, R^2 , the value of which affects the degree of convergence between the approximation function and the applied range of the approximated experimental curve. The higher the correlation coefficient is, the higher the accuracy of the applied approximation process can be observed. In the applied approx-

imation for the experimental equilibrium paths of the structure, the minimum correlation coefficient was set to $R^2 \geq 0.95$.

3.3. Numerical analysis

The study of stability and post-critical state was also conducted numerically by the finite element method using the commercial ABAQUS® simulation software. The scope of the numerical computations involved performing analyses of both critical and weakly post-critical states up to a value of approx. 150% of the lowest determined critical force. The analysis of the critical state involved solving a linear eigenproblem, leading to determination of the lowest critical load and the corresponding mode of stability loss. The eigenproblem is solved using the extreme potential energy conditions, i.e. the system's equilibrium is equal to the minimum potential energy [1]. This means that, in static systems, the second variation of potential energy must be positive. The second stage of the computations involved a nonlinear static analysis performed on a model with initial geometric imperfection corresponding to the lowest buckling mode with the amplitude equal to 0.1 of the profile wall thickness. This enabled determination of the post-critical equilibrium path of the structure describing the relationship between load and profile wall deflection in the normal direction $P-w$ for a weakly post-critical range. The geometrically nonlinear problem (large displacements) was solved by the Newton-Raphson method [1].

The discretization of the numerical model was performed using SHELL elements having 6 degrees of freedom in each node. We used 8-node S8R elements described by a second-order shape function and reduced integration. The technique of reduced integration is one of the oldest approximation methods for solving problems regarding displacement and stress in elements. Reduced integration enables rejecting false modes of finite elements deformation owing to the use of higher order polynomials to describe the element shape function [7, 11, 12, 22, 24, 30]. The discretization process was performed using a structural mesh of finite elements, with the side of the element set to 2 mm. With the applied discretization methods, it was possible to uniformly divide individual walls of the profile, thereby obtaining a numerical model consisting of 5760 finite elements and 17585 nodes. A general view of the numerical model is shown in Fig. 3b.

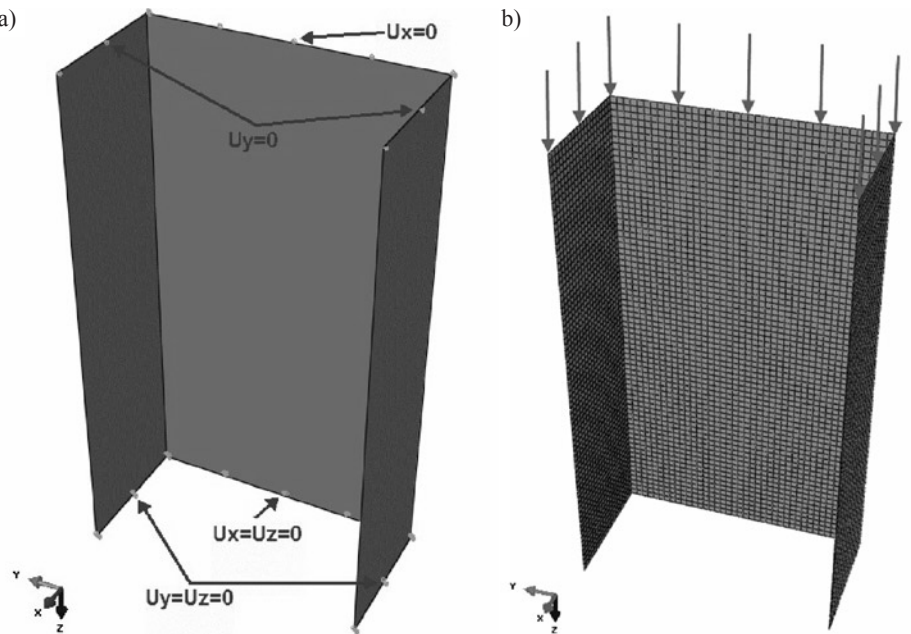


Fig. 3. Discrete model of a channel-section column: a) boundary conditions, b) discretization of the geometric model

The finite element used in the discretization process was a laminar element enabling defining the laminate structure based on the element's thickness. In the developed numerical model, the material is assigned orthotropic properties in two-dimensional state of stress, described by the experimentally determined mechanical properties of the composite material (Table 1).

The boundary conditions formulated for the numerical model ensured articulated support of the compressed composite columns – Fig. 3a. The boundary conditions were ensured by applying zero displacements to the nodes located on the edges of the lower and upper sections of the column, perpendicularly to the plane of each wall (displacements $u_x = 0$ and $u_y = 0$). In addition, the nodes from the bottom end of the column were blocked to prevent vertical displacement ($u_z = 0$), while the nodes belonging to the edge of the top end of the column were described by the same displacement $u_z = const$ via coupling the displacements relative to the axis of the column. The numerical model was subjected to load applied to the edge of the upper section of the column, ensuring that the column was under uniform compression in the axial direction.

4. Results and discussion

The experiments on the axially compressed thin-walled channel-section column provided information enabling the assessment of strains in the real structure in a function of external load. The results enabled performing qualitative and quantitative analyses of the pre-critical and critical states based on the recorded test parameters. The critical state was identified based on the obtained buckling mode and its corresponding critical load. The experimentally determined critical values served as a basis for verifying the FEM numerical results.

The investigation of the pre-critical and critical behaviour revealed that the lowest critical load corresponds to the local mode of stability loss of the structure resulting in formation of one half-wave on the walls and on the web of the channel-section profile. The lowest buckling mode obtained in the experiments and the numerical simulations is shown in Fig. 4.

The experimental and numerical results of buckling modes of the investigated channel-section column under compression show complete agreement. The measurements of strains per-

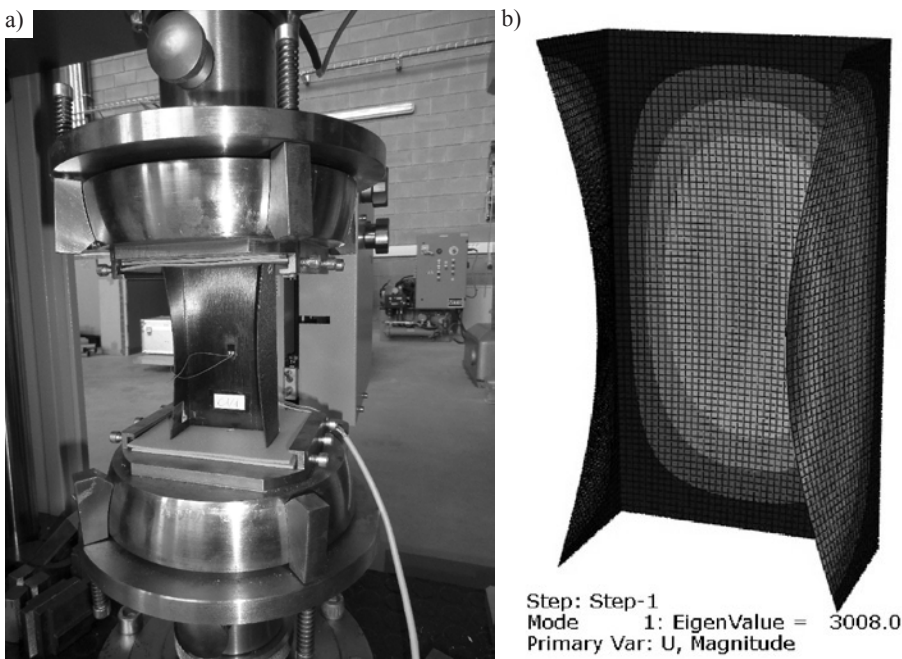


Fig. 4. Lowest buckling mode in a channel-section column: a) experiment, b) FEM

formed using resistance strain gauges enabled determination of the post-critical equilibrium path describing the relationship between the compressive force and the difference in strains $P-(\varepsilon_1 - \varepsilon_2)$. The obtained characteristics served as a basis for determining the critical load by two independent approximation methods: Koiter's method and the $P-w^2$ method. The key problem with such an approach is to select an adequate measuring range for describing the post critical path, which directly affects the results. With inadequate approximation procedures the experimental critical loads significantly differ from the numerical findings. In addition, the approximation range should be selected such so as to maintain the highest possible correlation coefficient R^2 in order to ensure sufficient accuracy of matching the approximation function to the experimental curve. In the simulations, the range of the approximated experimental curve in all investigated cases covered a part of the experimental post-critical path from the intersection point of force – strain to the end of the curve determined in the experiments for a weakly post-critical state (Koiter's method) or for a linear state ($P-w^2$ method), at the same time maintaining a high value of the correlation coefficient ($R^2 > 0.95$).

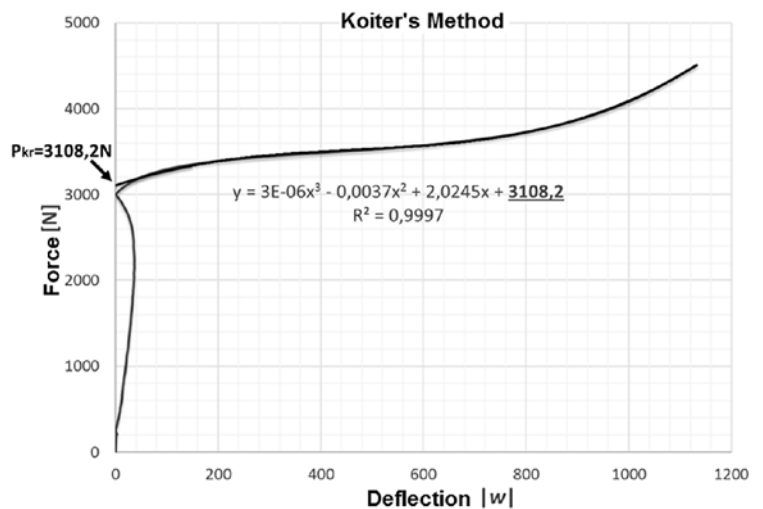


Fig. 5. Critical load determined by Koiter's method

As for the Koiter method, we examined the experimental post-critical equilibrium path expressed as $P-w$ (where deflection is determined according to $w \approx (\varepsilon_1 - \varepsilon_2)$), and then performed approximation using a third-order polynomial. The critical load was determined here as a point of intersection between the approximation function and the chart's vertical axis (axis of load). The critical load determined by Koiter's method is 3108.2 N – Fig. 5.

As for the $P-w^2$ method, we analyzed the post-buckling equilibrium path expressed as $P-(\varepsilon_1 - \varepsilon_2)^2$ and approximated by a linear function. Also here, the critical load is determined as the ordinate of a point of intersection between the straight line of approximation and the vertical axis in the chart (axis of load). The critical load determined by the $P-w^2$ method is 3125.8 N – Fig. 6.

The critical load determined by the above approximation methods was compared with the lowest eigenvalue determined numerically in the critical behaviour analysis. The critical load of the numerical model is 3008 N. All values

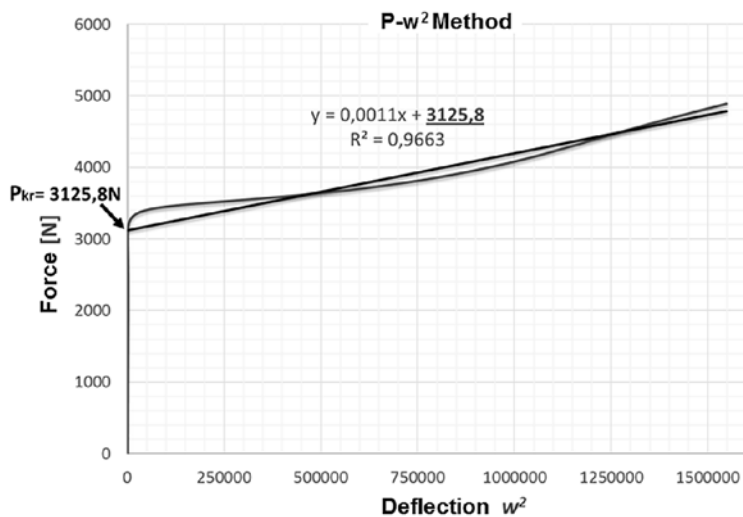


Fig. 6. Critical load determined by $P-w^2$ method

Table 2. Critical load – comparison of experimental and numerical results

FEM [N]	Koiter's method [N]	Koiter's/ FEM difference [%]	$P-w^2$ method [N]	$P-w^2$ / FEM difference [%]
3008	3108.2	3.3	3125.8	3.9

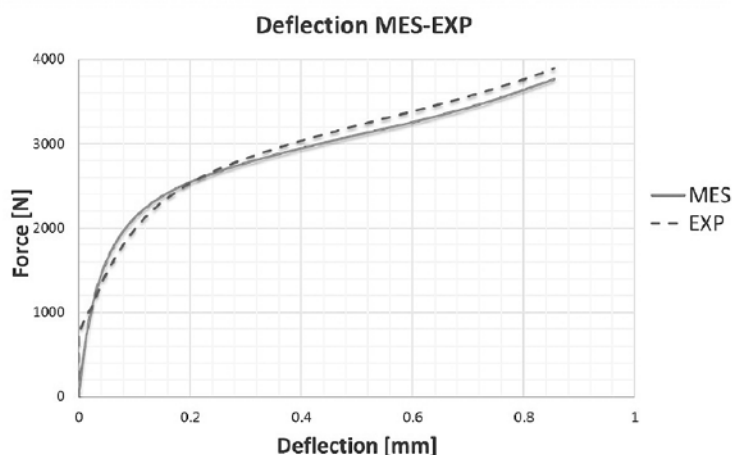


Fig. 7. FEM post-critical equilibrium paths

of the critical load determined by the applied research methods are listed in Table 2.

The values of the critical load describing the buckling of a thin-walled channel-section column determined by the approximation and

numerical methods show high agreement. The highest differences do not exceed 4%, which means that there is a high quantitative agreement between the applied research methods, and at the same time this confirms that the proposed procedure for calculating the critical load of a real structure was correct.

The post-critical equilibrium paths $P-w$ (compressive force – highest deflection perpendicular to the wall of the profile) determined for the weakly post-critical range are compared, too. The experimental results shown in Fig. 7 show both quantitative and qualitative agreement with the numerical results determined by the finite element method. The results confirm the adequacy of the developed numerical model for investigating the critical and post-critical behaviour of channel-section composite profiles under compression.

5. Conclusions

The study investigated the behaviour of a thin-walled channel-section column subjected to uniform compression. The critical load was determined based on the experimental results of the post-critical equilibrium paths of the structure obtained by two independent approximation methods: Koiter's method and the $P-w^2$ method. The experimental results were compared with the critical load determined by the finite element method. It was found that the results of critical load show a very high agreement, with the greatest differences not exceeding 4%. This confirms the possibility of using the proposed procedure to determine the critical load for real structures. Accurate determination of the critical load of thin-walled structures is extremely vital due to operational reasons, as it prevents the structure from undesired loss of stability.

The results reveal a high sensitivity of the approximation parameters on the results accuracy. In particular, this pertains to selecting an appropriate approximation range and a high value of the correlation coefficient R^2 to ensure agreement between the experimental characteristics of the structure and the approximation function.

The results reveal a high qualitative and quantitative agreement between the experimental results and the numerical findings. This concerns both the mode of stability loss of the structure, critical load, as well as the post-critical equilibrium paths $P-w$ in the early post-critical range. Therefore, the results provide vital information regarding the modelling of thin-walled composite structures and at the same time they confirm the correctness of the developed numerical models with respect to the eigenproblem and nonlinear statistical analysis in the post-critical range.

References

1. Abaqus HTML Documentation, 2016.
2. Adams DF, Carlsson LA, Pipes RB. Experimental characterization of advanced composite materials. CRC Press LLC, 2003.
3. Altenbach H, Altenbach J, Kissing W. Structural analysis of laminate and sandwich beams and plates. An introduction into the mechanics of composite. Lubelskie Towarzystwo Naukowe, 2001.
4. Banat D, Mania R.J. Comparison of failure criteria application for FML column buckling strength analysis. Composite Structures 2016; 140: 806-815, <http://dx.doi.org/10.1016/j.compstruct.2016.01.024>.
5. Bazant ZP, Cedolin L. Stability of Structures. Elastic, Inelastic, Fracture and Damage Theories. Oxford University Press UK 2010, <http://dx.doi.org/10.1142/7828>.
6. Bloom F, Coffin D. Handbook of thin plate buckling and postbuckling. CHAPMAN & HALL/CRC Boca Raton, London, New York, Washington, D.C. 2001.
7. Debski H, Sadowski T. Modelling of microcracks initiation and evolution along interfaces of the WC/Co composite by the finite element method. Computational Materials Science 2014; 83: 403-411, <http://dx.doi.org/10.1016/j.commatsci.2013.11.045>.

8. Debski H, Teter A, Kubiak T. Numerical and experimental studies of compressed composite columns. *Composite Structures* 2014; 118: 28-36, <http://dx.doi.org/10.1016/j.compstruct.2014.07.033>.
9. Doyle JF. *Nonlinear analysis of thin-walled structures*. Springer, 2001, <http://dx.doi.org/10.1007/978-1-4757-3546-8>.
10. Falkowicz K, Ferdynus M, Debski H. Numerical analysis of compressed plates with a cut-out operating in the geometrically nonlinear range. *Eksploracja i Niezawodność - Maintenance and Reliability* 2015; 17(12): 222-227, <http://dx.doi.org/10.17531/ein.2015.2.8>.
11. Fedorko G, Stanova E, Molnar V, Husakova N, Kmet S. Computer modelling and finite element analysis of spiral triangular strands. *Adv. Eng. Softw* 2014; 73: 11–21, <http://dx.doi.org/10.1016/j.advengsoft.2014.02.004>.
12. Ferdynus M. An energy absorber in the form of a thin-walled column with square cross-section and dimples. *Eksploracja i Niezawodność - Maintenance and Reliability* 2013; 15: 253-258.
13. Kolakowski Z, Mania RJ. Semi-analytical method versus the FEM for analyzing of the local post-buckling of thin-walled composite structures. *Composite Structures* 2013; 97: 99–106, <http://dx.doi.org/10.1016/j.compstruct.2012.10.035>.
14. Kolakowski Z. Static and dynamic interactive buckling of composite columns. *Journal of Theoretical and Applied Mechanics* 2009; 47: 177-192.
15. Kopecki T, Bakunowicz J, Lis T. Post-critical deformation states of composite thin-walled aircraft load-bearing structures. *Journal of Theoretical and Applied Mechanics* 2016; 54(1): 195-204, <http://dx.doi.org/10.15632/jtam-pl.54.1.195>.
16. Kopecki T, Mazurek P, Lis T, Chodorowska D. Post-buckling deformation states of semi-monocoque cylindrical structures with large cut-outs under operating load conditions. Numerical analysis and experimental tests. *Eksploracja i Niezawodność - Maintenance and Reliability* 2016; 18(1): 16-24, <http://dx.doi.org/10.17531/ein.2016.1.3>.
17. Parlapalli MR, Soh KC, Shu DW, Ma G. Experimental investigation of delamination buckling of stitched composite laminates. *Composites, Part A* 2007; 38: 2024–2033, <http://dx.doi.org/10.1016/j.compositesa.2007.05.001>.
18. Paszkiewicz M, Kubiak T. Selected problems concerning determination of the buckling load of channel section beams and columns. *Thin-Walled Structures* 2015; 93: 112-121, <http://dx.doi.org/10.1016/j.tws.2015.03.009>.
19. PN EN ISO 527-4 Oznaczanie właściwości mechanicznych przy statycznym rozciąganiu. Warunki badań kompozytów tworzywowych izotropowych i ortotropowych wzmocnionych włóknami."
20. PN EN ISO 14126 Kompozyty tworzywowe wzmocnione włóknem. Oznaczanie właściwości podczas ściskania równoległe do płaszczyzny laminowania."
21. PN EN ISO 14129 Kompozyty tworzywowe wzmocnione włóknem. Oznaczenie naprężenia ścinającego i odpowiadającego odkształcenia, modułu ścinania i wytrzymałości podczas rozciągania pod kątem $\pm 45^{\circ}$."
22. Rudawska A, Debski H. Experimental and numerical analysis of adhesively bonded aluminium alloy sheets joints. *Eksploracja i Niezawodność - Maintenance and Reliability* 2011; 1: 4-10.
23. Singer J, Arbocz J, Weller T. *Buckling experiments. Experimental methods in buckling of thin-walled structure. Basic concepts, columns, beams, and plates*. New York: John Wiley & Sons Inc, 1998; 1 (2002; 2).
24. Stanova E, Fedorko G, Kmet S, Molnar V, Fabian M. Finite element analysis of spiral strands with different shapes subjected to axial loads. *Adv. Eng. Softw.* 2015; 83: 45–58, <http://dx.doi.org/10.1016/j.advengsoft.2015.01.004>.
25. Taheri F, Nagaraj M, Khosravi P. Buckling response of glue-laminated columns reinforced with fiber-reinforced plastic sheets. *Composite Structures* 2009; 88: 481–90, <http://dx.doi.org/10.1016/j.compstruct.2008.05.013>.
26. Teter A, Debski H, Samborski S. On buckling collapse and failure analysis of thin-walled composite lipped-channel columns subjected to uniaxial compression. *Thin-Walled Structures* 2014; 85: 324-331, <http://dx.doi.org/10.1016/j.tws.2014.09.010>.
27. Tsai SW, Wu EM. A general theory of strength for anisotropic materials. *J. Compos. Mater* 1971: 58–80, <http://dx.doi.org/10.1177/002199837100500106>.
28. Turvey GJ, Zhang Y. A computational and experimental analysis of the buckling, postbuckling and initial failure of pultruded GRP columns. *Computers & Structures* 2006; 84: 1527–1537, <http://dx.doi.org/10.1016/j.compstruc.2006.01.028>.
29. Wong PMH, Wang YC. An experimental study of pultruded glass fibre reinforced plastics channel columns at elevated temperatures. *Composite Structure* 2007; 81: 84–95, <http://dx.doi.org/10.1016/j.compstruct.2006.08.001>.
30. Zienkiewicz OC, Taylor R.L. *Finite Element Method (5th Edition) Volume 2 – Solid Mechanics*. Elsevier, 2000.

Paweł WYSMULSKI

Hubert DĘBSKI

Patryk RÓŻYŁO

Katarzyna FALKOWICZ

Mechanical Engineering Faculty

Lublin University of Technology

ul. Nadbystrzycka 36, 20-618 Lublin, Polska

E-mails: p.wysmulski@pollub.pl, h.debski@pollub.pl, p.rozylo@pollub.pl,

k.falkowicz@pollub.pl
